Supplementary Information (SI) for Journal of Materials Chemistry B.

Supporting Information

Ice templating water-stable macroporous polysaccharide hydrogels to mimic plant stems

*Katsuya KOMIYAMA [1], Maya ALLARD [1], Corentin ESCHENBRENNER [1], Clémence SICARD [2,3], Ahmed HAMRAOUI [1,4] Francisco M. FERNANDES [1]**

[1] Sorbonne Université, UMR 7574, Laboratoire de Chimie de la Matière Condensée de Paris,
75005, Paris, France

[2] Université de Versailles Saint-Quentin-en Yvelines, UMR 8180, L'Institut Lavoisier de Versailles, 78035, Versailles, France

[3] Institut Universitaire de France

[4] Université Paris Cité, CNRS, UMR8003, Saints Pères Paris Institute for the Neurosciences, 45, rue des Saints-Pères, 75006 Paris, France

* Corresponding author. E-mail: francisco.fernandes@sorbonne-universite.fr; Tel: +33 1 44 27 62 45

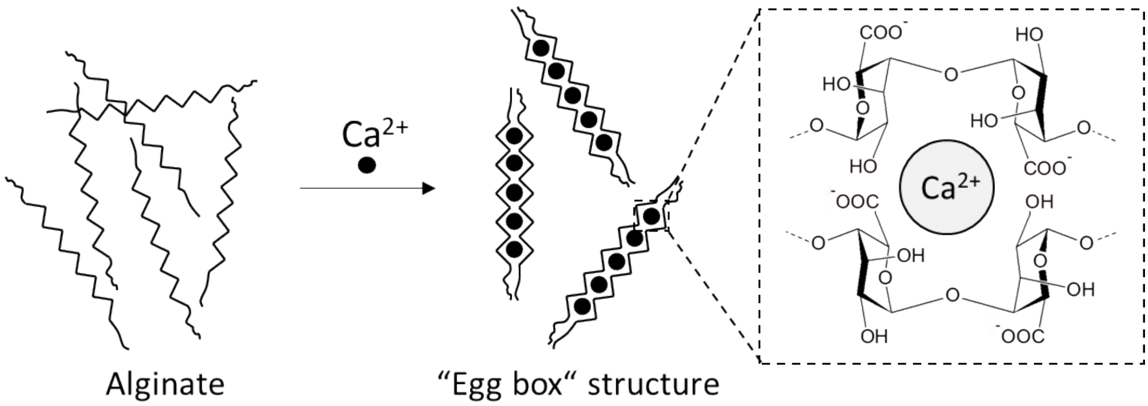

Figure S1. Egg-box structure of alginate gel in the presence of Ca^{2+}.

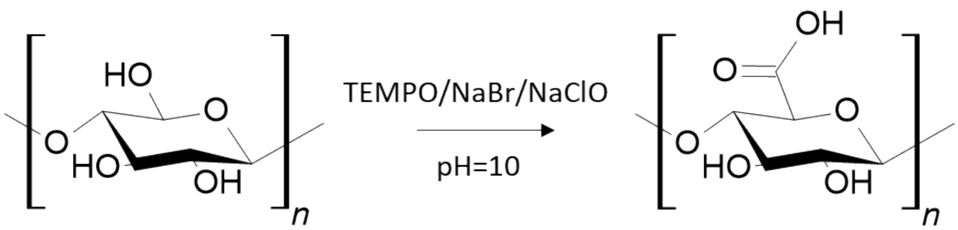

Figure S2. Scheme of TEMPO oxidation of cellulose.

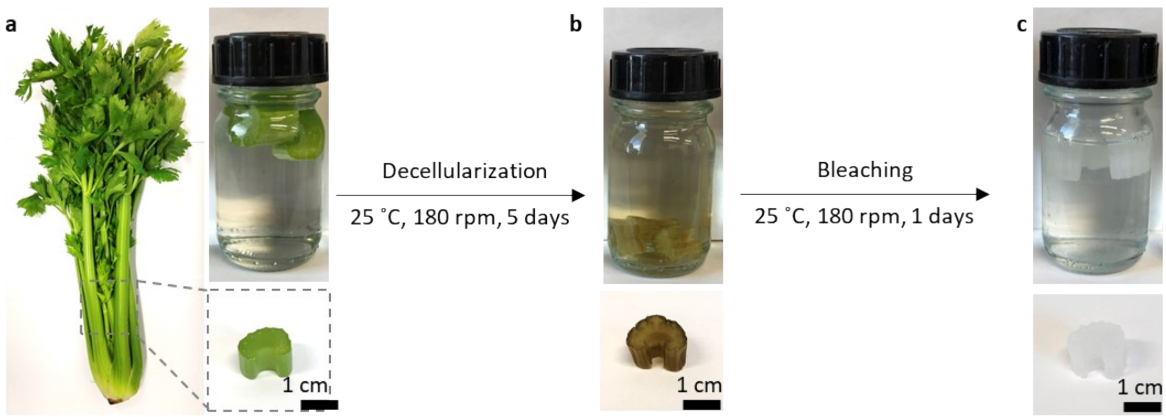

Figure S3. The scheme of the decellularization and bleaching for the celery (*Apium graveolens*), (a) The stem of the celery was cut into 1 cm and then (b) cut samples was immersed in 10 % SDS solution for 5 days. (c) After 5 days decellularization, samples are immersed in NaClO solution for 1 day for bleaching.

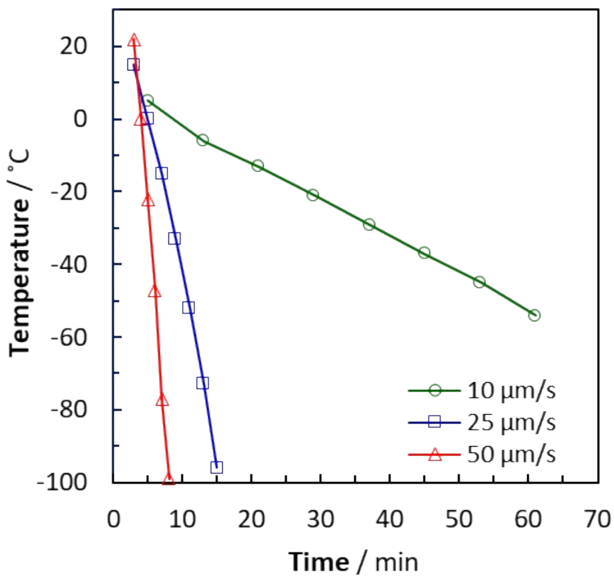

Figure S4. 3 cooling temperature profiles applied in this study for the unidirectional ice-templating, resulting in constant ice-front velocity of 10, 25 and 50 µm/s.

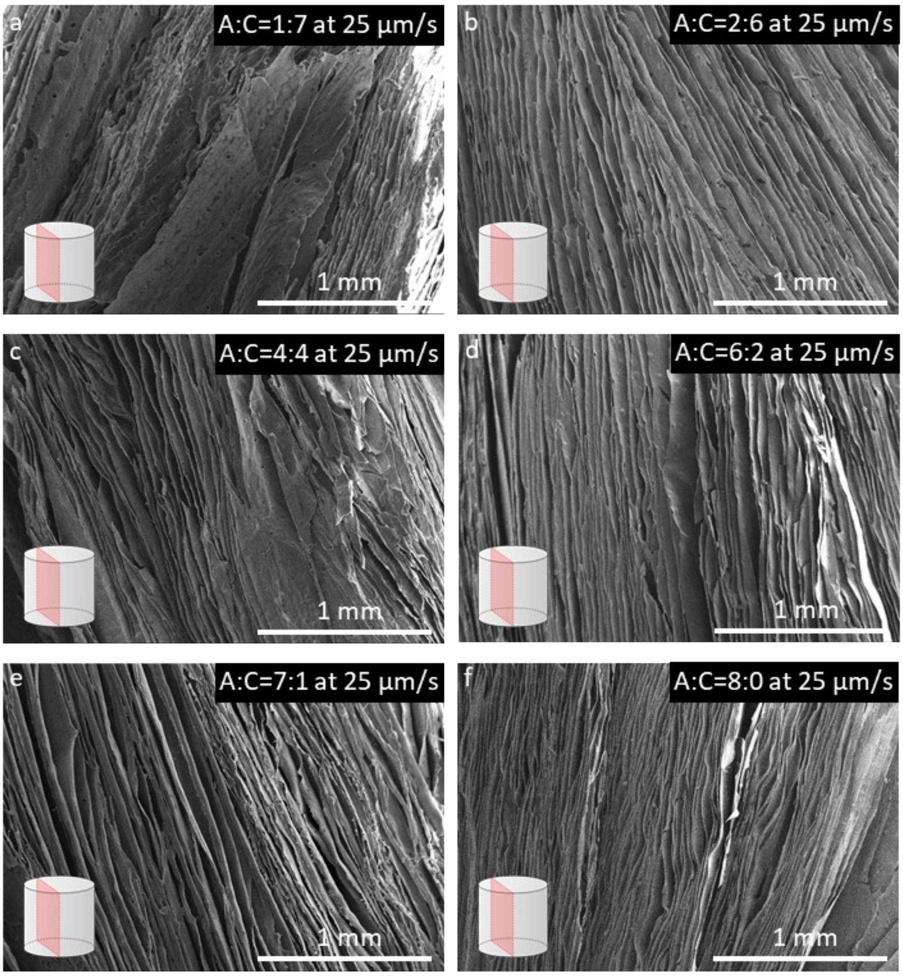

Figure S5. SEM images in longitudinal section of Ca-crosslinked hydrogels with the different ratio of alginate and oxidized cellulose prepared at constant ice growth velocity (25 µm/s). (a) A:C=8:0, (b) A:C=7:1, (c) A:C=6:2, (d) A:C=4:4, (e) A:C=2:6, and (f) A:C=1:7.

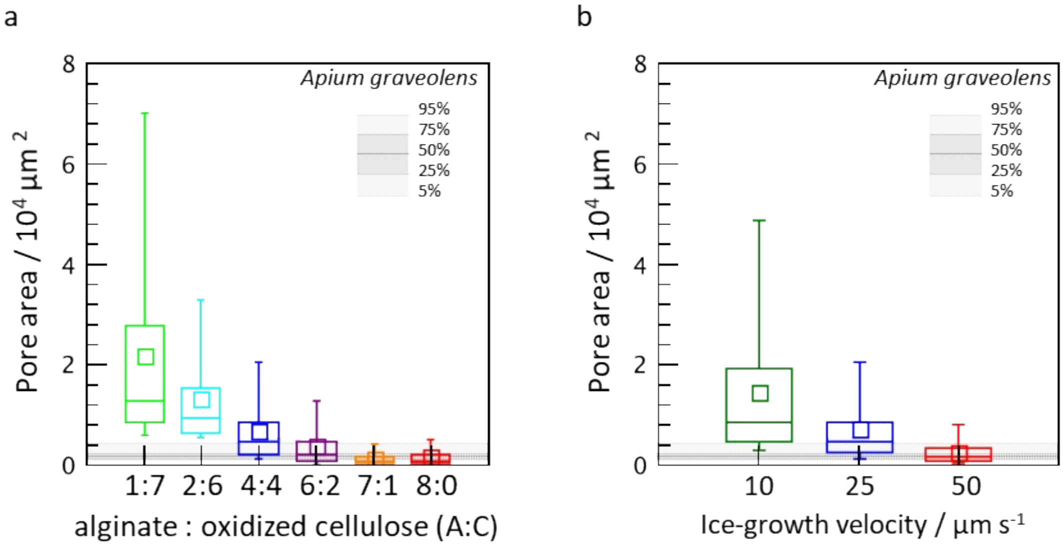

Figure S6. Normal scale pore distribution. (a) Summary of the pore area distribution of alginate and oxidized cellulose macroporous hydrogels at different compositions for 25 µm/s (ice growth velocity). (b) Summary of the pore area distribution of alginate and oxidized cellulose macroporous hydrogels (A:C=4:4) at different ice front velocities. Moustaches delimit the 5 and 95 percentiles of the distribution and box limits represent the 1st and 3rd quartiles. Gray horizontal bars depict the pore size distribution of *A. graveolens* xylem vascular system.

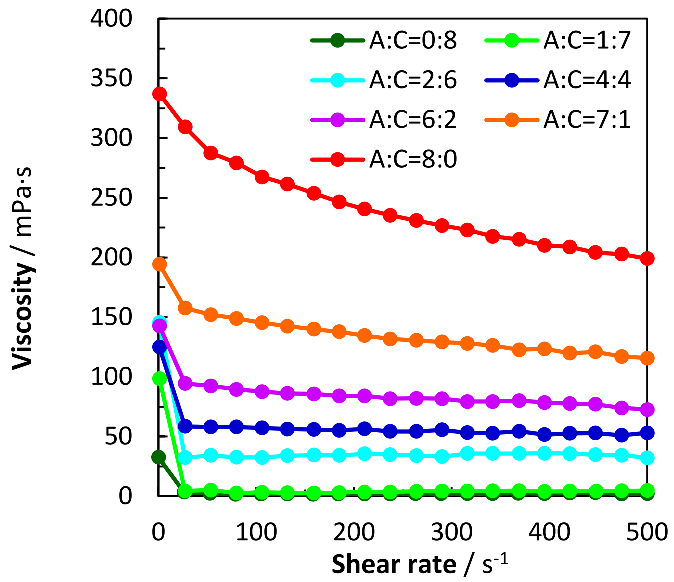

Figure S7. Viscosity profile of the suspensions with different ratio of alginate and oxidized cellulose.

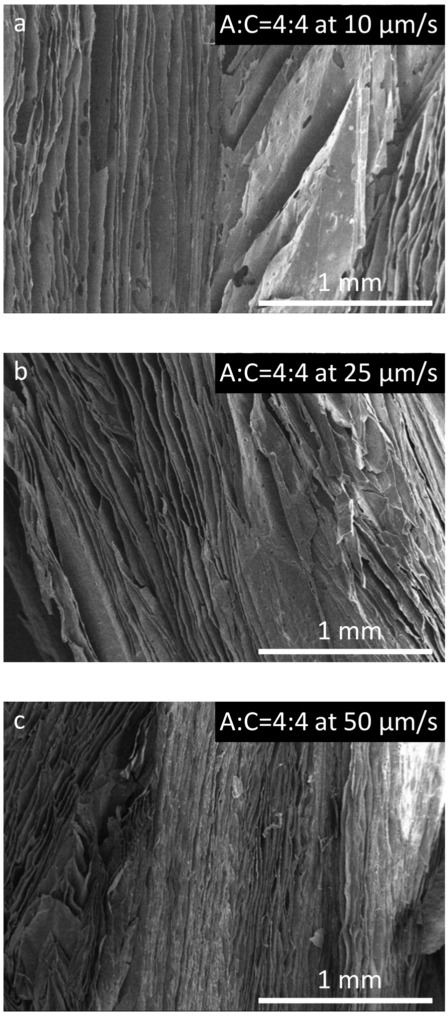

Figure S8. SEM images in longitudinal section of Ca-crosslinked hydrogels prepared at different ice growth velocity (10, 25, and 50 µm/s) at constant ratio of alginate and oxidized cellulose (4:4). (a) v = 10 µm/s, (b) v = 25 µm/s, and (c) v = 50 µm/s.

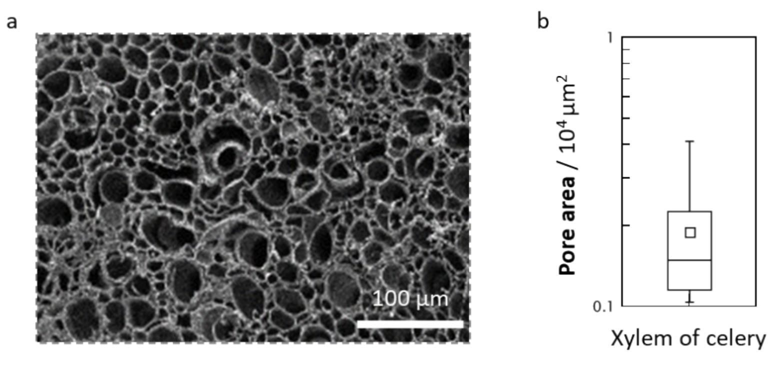

Figure S9. (a) SEM image of celery xylem and (b) its pore area distribution.

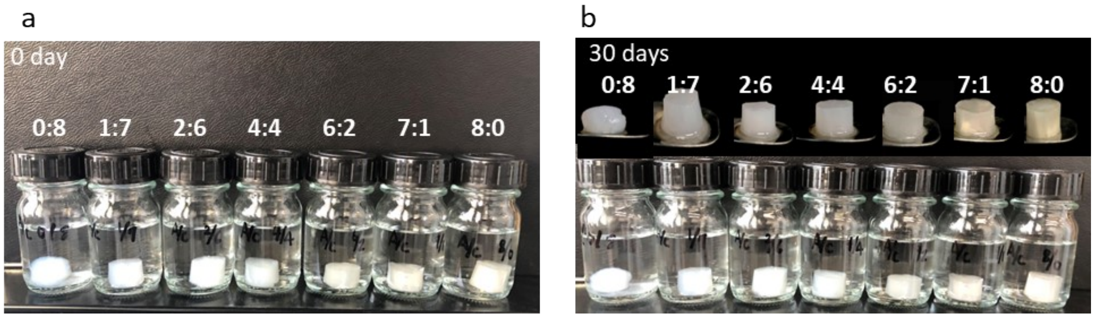

Figure S10. Photos of water stability tests of ion-crosslinked samples with the different ratio of alginate and oxidized cellulose (prepared with an ice growth velocity of 25 μm/s); (a) immediately after the immersion in the water, (b) 30 days after the immersion.

Table S1. Mechanical properties of hydrogels with an ice growth velocity of 25 μm/s with different compositions of alginate/oxidized cellulose (A:C) after ion-crosslinking.

	Young's modulus / MPa	**Toughness** / J/m^3	**Yield stress** / KPa	**Compression stress** $_{ε=20\%}$ / KPa	**Compression stress** $_{ε=40\%}$ / KPa	**Compression stress** $_{ε=60\%}$ / KPa
0:8	0.003 ± 0.001	0.04 ± 0.01	0.7 ± 0.2	0.3 ± 0.1	0.8 ± 0.2	1.6 ± 0.5
1:7	0.008 ± 0.003	0.08 ± 0.02	0.8 ± 0.3	1.0 ± 0.1	1.8 ± 0.2	3.8 ± 0.8
2:6	0.032 ± 0.017	0.15 ± 0.03	1.5 ± 0.2	2.1 ± 0.4	2.7 ± 0.5	5.3 ± 1.1
4:4	0.034 ± 0.015	0.23 ± 0.05	3.4 ± 1.1	3.9 ± 0.9	4.4 ± 0.8	6.1 ± 1
6:2	0.070 ± 0.017	0.31 ± 0.05	4.1 ± 0.9	5.1 ± 1	5.8 ± 0.9	8.4 ± 1.1
7:1	0.084 ± 0.019	0.40 ± 0.05	6.0 ± 0.9	6.5 ± 0.9	7.3 ± 0.6	11.4 ± 1.5
8:0	0.096 ± 0.036	0.39 ± 0.08	5.0 ± 1.5	5.8 ± 1.3	7.5 ± 1.3	10.8 ± 1.9

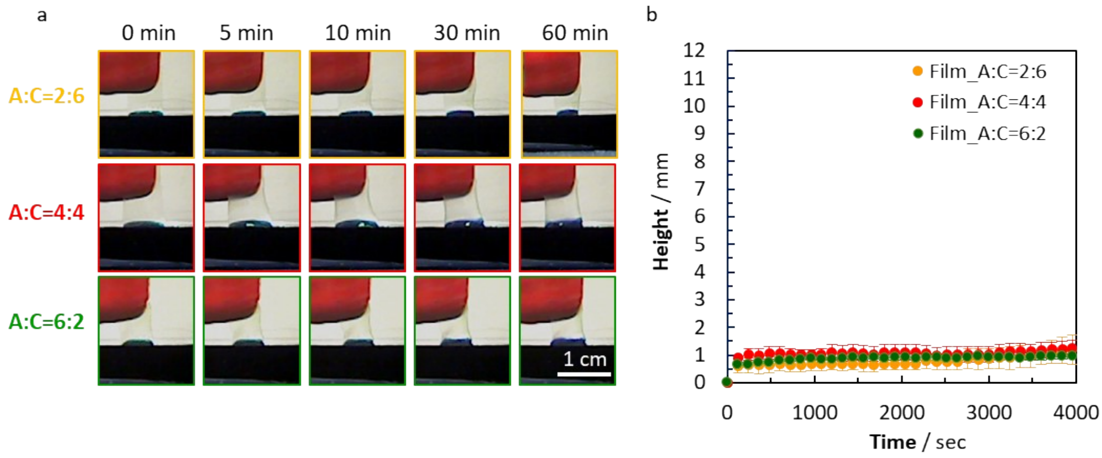

Figure S11. Liquid transport experiment using the films with different compositions of alginate and oxidized cellulose. (a) Optical photos showing capillary action behavior. (b) Time-liquid height curves.

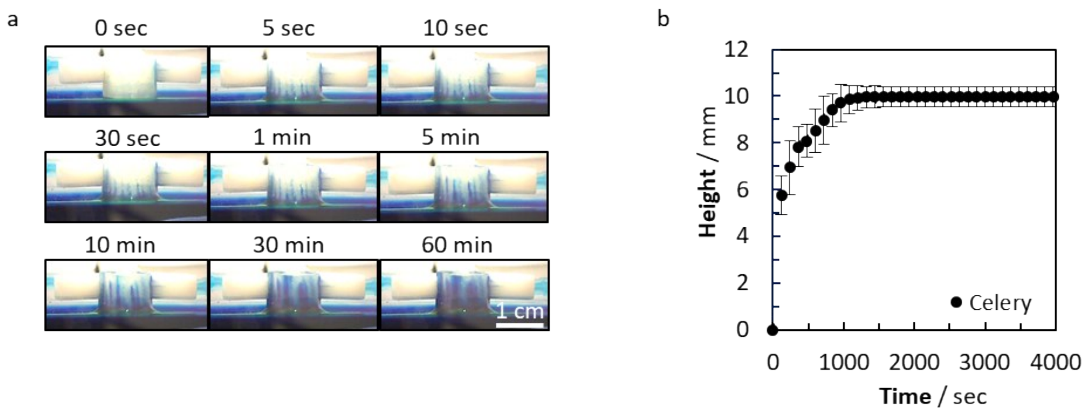

Figure S12. Liquid transport experiment with celery. (a) Optical photos showing capillary action behavior. (b) Time-liquid height curves and rising speeds of celery.

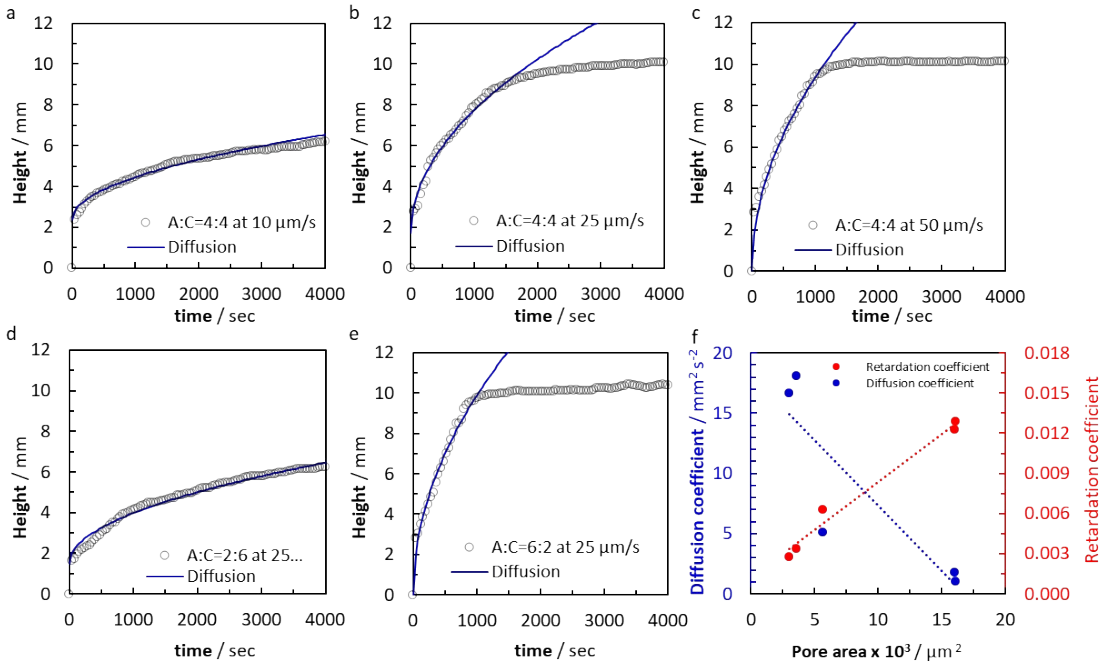

Figure S13. Capillary water transport behavior of hydrogels prepared with different ice-growth velocities (a-c) and different compositions of alginate and oxidized cellulose (d and e) and those theoretical curves fitting to the equation of mean square displacement (i.e. $h(t)^2=6Dt$), (f) trends among pore area, diffusion coefficients, and retardation coefficients. Dashed lines are a guide to the eye.